Journal of Quantitative Spectroscopy & Radiative Transfer 113 (2012) 2081–2087

Contents lists available at SciVerse ScienceDirect

Journal of Quantitative Spectroscopy & Radiative Transfer

journal homepage: www.elsevier.com/locate/jqsrt

Vibrational relaxation and vibration-rotation energy transfer between highly vibrationally excited KH($X^1\Sigma^+$, $v=14$–21) and CO_2

Xiu-hua Cui [a,b], Bao-xia Mu [b], Yi-fan Shen [b,*], Kang Dai [b]

[a] School of Science, Xi'an Jiaotong University, Xi'an 710049, China
[b] School of Physics, Xinjiang University, Urumqi 830046, China

ARTICLE INFO

Article history:
Received 19 March 2012
Received in revised form
11 June 2012
Accepted 13 June 2012
Available online 28 June 2012

Keywords:
Energy transfer
Overtone pump
Rotational temperature
Doppler-profile
KH
CO_2

ABSTRACT

The vibrational levels of KH($X^1\Sigma^+$, $v''=0$–3) were generated in the reaction of K (5P) and H_2. Vibrational state total relaxation rate coefficients$k_{v''}(CO_2)$ for KH ($v''=14$–21) are measured in an overtone pump-probe configuration. The rate coefficient $k_{v''}(CO_2)$ is strongly dependent on vibrational quantum number. Scattered CO_2 (00^00, $32\leq J\leq 48$) molecules were excited to CO_2 (10^05, $J+1$) states. The rotational temperatures of CO_2 (00^00, $J=32$–48) states populated by collisions with highly vibrationally excited KH ($v''=14$–21) are obtained. The average rotational energy of the scattered CO_2 molecules is increased by a factor of 2.33 when KH level $v''=14$ increases to $v''=21$. The average translational energy of the scattered CO_2 molecules is increased roughly linearly as a function of CO_2 J state. Under single collision conditions, state-specific energy transfer rate coefficients for collisions of highly excited KH with CO_2 are obtained. For $v''=19$, the integrated rate coefficients k_{int} increases by a factor of 4.5 to $v''=14$.

Introduction

The collisional quenching of highly vibrationally excited molecules and the subsequent redistribution of energy are of fundamental importance for understanding of energy transfer dynamics. Collisional energy transfer of high-energy molecules is a key step in many chemical processes but fundamental questions remain unanswered [1–3]. One question is how the amount of vibrational energy in the highly excited molecule affects the energy transfer in terms of product energy partitioning and energy transfer rates. Currently, there are no models for predicting how large vibrationally excited molecules lose their energy through strong collisions. The dynamics of strong collisions of highly excited molecules with CO_2 has been well documented for a number of highly excited donor molecules using high-resolution IR probing [4–6]. The energy dependence of collisional quenching of high-energy donor molecules, pyridine (C_5H_5N) and pyrazine ($C_4H_4N_2$) with CO_2 has been investigated with state-resolved probing [7–9], but these studies were limited to rather small ranges of donor energies, corresponding to a 10% and 30% increase in energy, respectively. Mullin and co-workers have used high resolution transient IR absorption to investigate the strong collisions of azulene (C_8H_{10}) with CO_2 for two initial energies, $E=20{,}390$ and $38{,}580\ cm^{-1}$ [10]. Their study shows that both the distribution of transferred energy and energy transfer rates are sensitive to the azulene energy. The average rotational and translational energies of the scattered CO_2 molecules are double when the azulene energy is increased by a factor of 2. The rate of energy transfer in strong collisions is increased nearly by a factor of 4 when the azulene energy is doubled.

For diatomic molecules excited with a large amount of vibrational energy, fully quantum state resolved experiments are possible, and the quantum mechanical

* Corresponding author. Tel.: +86 018999919722; +86 0991 8582187; fax: +86 0991 8582405.
E-mail addresses: xjcxh0991@xju.edu.cn (X.-h. Cui), shenyifan01@xju.edu.cn (Y.-f. Shen).

0022-4073/$ - see front matter © 2012 Elsevier Ltd. All rights reserved.
http://dx.doi.org/10.1016/j.jqsrt.2012.06.021

identities of all excited states are unambiguous. Connection to rigorous theoretical calculations can also be accomplished. For these reasons, the collisional dynamics of highly vibrationally excited diatoms is an interesting research area as it offers a bridge between experiments at low and high vibrational excitation. The investigation of small molecules has had an impact on understanding the mechanism of energy transfer in highly vibrationally excited molecules. Wodtke and co-workers [11,12] have employed the stimulated emission pumping (SEP) technique and applied it to prepare a single highly excited vibrational level of diatomic molecules. They have measured the rate coefficients for vibrational relaxation of O_2 ($X^3\sum_g^-$, v=15–26) by CO_2. The vibrational relaxation was dramatically enhanced (by about a factor of 100) near O_2 (v=18), where the 2–1 near resonant energy transfer process

$$O_2(v)+CO_2(000)\rightarrow O_2(v-2)+CO_2(001)$$

has a minimum energy defect of only a few cm^{-1} for $O_2(v=18)$. More direct evidences for the 2–1 resonance came from pump–dump–probe experiments in which O_2 (v=17) was prepared in mixture with CO_2 and the evolution of the population in v=16 and v=15 was observed. In those experiments population initially in v=17 skips to v=16 and appears in v=15. Similarly, 2–1 resonances were found for other systems [13,14].

In K–H_2 mixture, K (4S) is photoexcited to the 5P state that reacts with a hydrogen molecule. The KH molecule is formed in its electronic ground state [15–17]

$$K(5P)+H_2\rightarrow KH(v''=0-3)+H \quad (1)$$

Using overtone pumping, a pulse laser may generate high vibrational levels as

$$KH(X^1\Sigma^+,0)+h\nu\rightarrow KH(X^1\Sigma^+,v'') \quad (2)$$

In this work, we have performed measurements for determining vibrational-state-specific removal relaxation rate coefficients $k_{v''}(CO_2)$ for KH($X^1\Sigma^+$,v''=14–21), and found the strong vibrational level dependence. We have used high-resolution overtone spectroscopy of CO_2 at $\lambda\sim$780 nm to measure the nascent rotational and translational energy distributions for scattered CO_2 (00^00) molecules in high rotational states as a function of vibrational energy of KH($X^1\Sigma^+$). Based on our spectral measurements, absolute energy transfer rate coefficients are reported.

Experimental methods

The experimental setup is shown in Fig. 1. The reaction cell was a five-arm crossed heat-pipe oven, four arms formed a planer cross and the fifth perpendicular arm containing a reservoir of potassium was sealed to the bottom of the intersection of the four arms. The cell was connected to a vacuum and gas-filling system, which allowed the cell to be evacuated and filled with variable gas pressures. The cell temperature was monitored by a thermocouple of intruding in the vicinity of the reaction regime. The K metal in the oven was heated to 450 K. The chamber was evacuated to 10^{-5} Torr prior to introduction

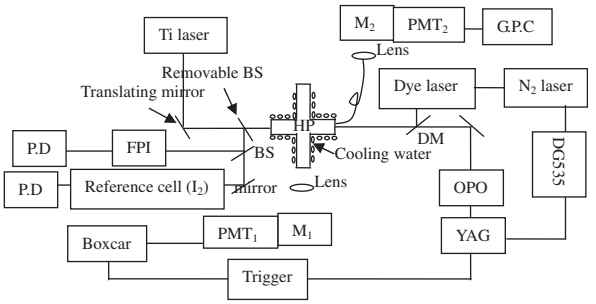

Fig. 1. Experimental setup. HP: heat pipe oven; OPO: optical parametric oscillator; M: monochromator; PMT: photomultiplier; G.P.C: gated photon counter; DM: dichroic mirror; P.D: photodiode; BS: beam splitter; FPI: Fabry–Perot interferometer.

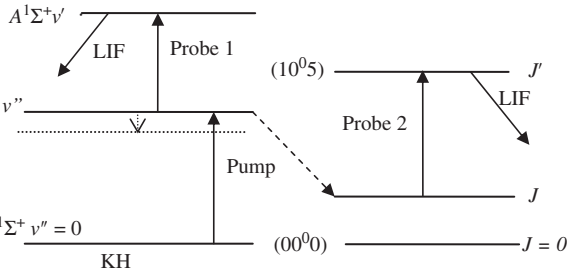

Fig. 2. Processes involved in the population and depopulation of KH and CO_2 level in this experiment.

of H_2 and CO_2. The H_2 pressure varied from 0.01 to 0.5 Torr. The CO_2 pressure varied from 0.01 to 24 Torr. H_2 gas was filled in the cell for use as a reaction gas. CO_2 gas was filled in the cell for use both as a collision partner with excited KH molecules and as a buffer gas which prevented K condensation on the cell windows.

A dye laser (ATM200) pumped by a N_2 laser (MNL200) was tuned to 404.4 nm for excitation of K (5P) state. KH($X^1\Sigma^+$,v''=0–3) were formed by K(5P)+H_2 reaction. A frequency-doubled 10 Hz Q-switched Nd: YAG laser was used to pump an OPO laser (Rainbow/NIR-D/S) (pump laser), which was used to excite KH from $X^1\Sigma^+(v''=0)$ to $X^1\Sigma^+(v''=14-21)$ states. The time delay between N_2 laser and OPO laser, controlled by a delay generator (DG535), was adjusted to be about 10 μs. During this time, KH (v''=1–3) molecules underwent a sufficient number of collisions to relax to KH (v''=0). A cw Ti-sapphire laser (COHERENT Inc. Verdi-G5) (probe laser) produces 450 mW of power with a linewidth of < 5 MHz. This laser was used as a probe to further excite the $X^1\Sigma^+(v'')$ states to the $A^1\Sigma^+(v')$ state. Highly vibrationally excited KH molecules were prepared by overtone pumping and laser induced fluorescence (LIF) was used to probe the KH($X^1\Sigma^+$,v'') molecules (see Fig. 2). LIF of $A^1\Sigma^+(v')\rightarrow X^1\Sigma^+(v'')$ transition was detected at right angles to the laser by a detector. It was a photomultiplier tube (RCAC31034, PMT_1) attached to the output of a monochromator (M_1) which resolution is 0.04 nm. The detector signal was fed into a boxcar averager-gated integrate system (SRS SR250). The averaged output was then recorded by a computer.

The highly excited KH is quenched through collisions with CO_2. This process can be written as

$$KH(X^1\Sigma^+, v_1'') + CO_2 \rightarrow KH(X^1\Sigma^+, v_2'' < v_1'') + CO_2(00^00, J) \quad (3)$$

Scattered nascent CO_2 (00^00) molecules in high rotational states were probed using the Ti-sapphire laser. The laser optical frequency was locked to the center of a single rovibrational transition of CO_2 using a static I_2 reference cell. The cell was a closed Pyrex glass cell that was warmed up to 350 K in order to have enough I_2 vapor pressure. The overtone fluorescence was collected using a fiber optic cable and transmitted to the monochromator (M_2). The fiber optic cable was placed adjacent to one of the cell windows at a point near where the dye laser beam entered the cell. The position of the fiber was such that the coupling lens observed the fluorescence along the path of the laser beams. This near 180° observation angle was used to ensure that the maximum amount of fluorescence was collected. The overtone fluorescence by scanning Ti-sapphire laser was measured by a SR400 gated photoncounter. The photoncounter was gated on by the laser pulses, each of which activated the counter for a time span about 1 μs. Doppler-broadened transition line profiles were collected to measure the nascent translational energy gain due to collisions. Transition line profiles were obtained by locking the Ti-sapphire laser to a fringe of a scanning Fabry–Perot interferometer and collecting transition signals as the interferometer was tuned over an individual transition line.

The technique we have developed goes beyond the usual pump-probe methodology which typically yields either time-averaged line shape information (when two cw lasers are used) or time-resolved populations without line shape information (when two pulsed lasers are used). By using a pulsed laser to excite KH (v'') to KH ($v''=14$–21) and then using a cw laser to probe the collisionally relaxed KH molecules. Timed excitation spectra are taken by scanning the cw probe laser over the $X^1\Sigma^+(v''J'') \rightarrow A^1\Sigma^+(v'J')$ transition while the boxcar gate is set to monitor $A^1\Sigma^+(v'J') \rightarrow X^1\Sigma^+(vJ)$ fluorescence. The time between the end of OPO laser pulse and the center of the boxcar detection window (which we will henceforth refer to as the "delay time") is varied for each scan in order to get a clear picture of the time evolution of the spectral line intensities and shapes.

Results and discussion

Vibrational relaxation rate coefficients

The OPO laser excited KH from $X^1\Sigma^+(v''=0, J''=6)$to $v''=14, J''=7$.The probe laser scanned (17, 14) A–X band. Fig. 3 shows LIF excitation spectrum of the (17, 11) A–X band obtained by scanning the probe laser wavelength. Assignment of the spectrum is easy since molecular constants for KH is known for both upper and lower states [18]. Neither Hönl–London nor Franck–Condon factors are taken into account because all lines are believed to be saturated. The ratio of the intensities of the rovibronic transitions is the ratio of the populations of the X ($v''=14, J''$) rovibronic states.

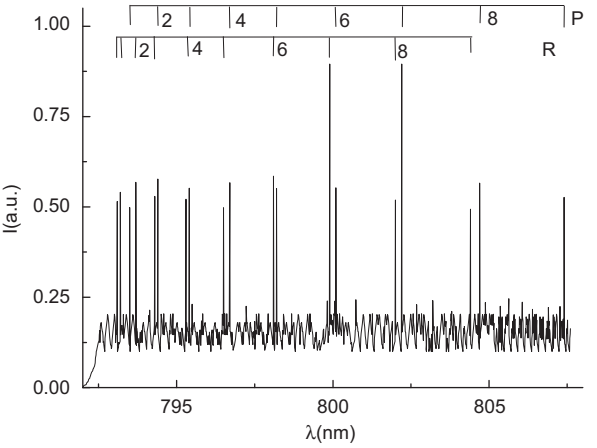

Fig. 3. LIF excitation spectra of the$A^1\Sigma^+(v'=17) \rightarrow X^1\Sigma^+(v''=11)$ band when $v''=14$ of ground state KH is prepared and (17–14) A–X band is scanned.

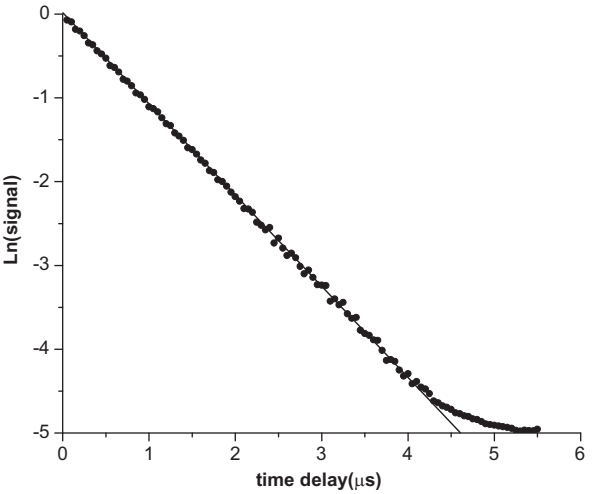

Fig. 4. Semilogarithmic plot for time-resolved fluorescence of KH in the $A^1\Sigma^+(17,8) \rightarrow X^1\Sigma^+(11,7)$transition when$X^1\Sigma^+(14,7)$is prepared ($P_{CO_2}=24$Torr,$P_{H_2}=0.5$Torr); The effective lifetime is 0.92 μs.

Fig. 4 shows the semilogarithmic plot for time-resolved fluorescence of the KH in $A^1\Sigma^+(17,8) \rightarrow X^1\Sigma^+(11,7)$ transition when X (14,7) is prepared. The typical number of data points in a time profile is 200, and the step size is varied (20 ns) according to the time scales of the profile. The slope yields a collisional lifetime. From such data collected at several pressures a Stern–Volmer plot can be constructed and a molecular relaxation rate coefficient can be extracted for the sum of all process that give rise to the decay of the prepared vibrational state. Several Stern–Volmer plots are shown in Fig. 5. The slope of the curves is proportional to the rate coefficient. The vibrational state dependent relaxation rate coefficients are tabulated in Table 1. The vibrational state specific rate coefficients reported here are average deactivation rate coefficients that have contributions from all the populated rotational states. The effect of radiative loss is negligible.

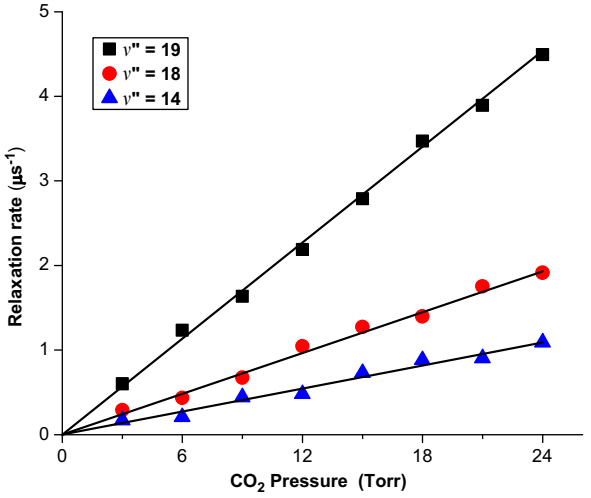

Fig. 5. Stern–Volmer plots for collisional quenching of vibrational states $v''=14$, 18 and 19.

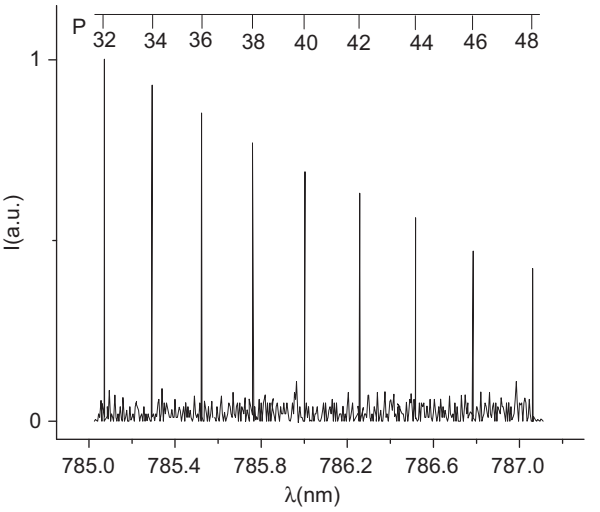

Fig. 6. LIF spectra of the $(10^{0}5) \leftarrow (00^{0}0)$ transition in CO_2+KH ($v''=14$) ($P_{CO_2}=15$ mTorr).

Table 1
Collisional relaxation rate coefficients (in 10^{-12} cm^3 molecule^{-1} s^{-1}) and cross sections (10^{-16} cm^2).

v''	Energy/cm^{-1}	Rate coefficient[a]	Cross section
14	11,319	1.3 ± 0.14	0.18
15	11,883	1.5 ± 0.17	0.21
16	12,475	1.7 ± 0.19	0.24
17	12,912	1.9 ± 0.21	0.27
18	13,368	2.3 ± 0.25	0.32
19	13,778	5.4 ± 0.59	0.76
20	14,134	4.5 ± 0.50	0.63
21	14,423	3.4 ± 0.37	0.48

[a] Numbers in the parentheses are 1σ errors.

CO_2 rotational energy gain from KH ($X^1\Sigma^+ v''$)–CO_2 collisions

Fig. 6 shows lasers induced fluorescence spectrum of $(10^{0}5)\leftarrow(00^{0}0)$ band obtained by scanning the probe laser wavelength at 1 μs following excitation of KH. The pertinent spectral assignments are identified by using the given coefficients [19,20] for $(10^{0}5)$ and $(00^{0}0)$ states of CO_2. This is the straightforward documentation of the high rotational CO_2 $(00^{0}0, J)$ products.

The fluorescence signals are converted to nascent CO_2 populations using absorption cross sections [20] and transition Doppler-broadened line widths described in the next section. Fig. 7 is a plot of the logarithm of the population of states J divided by the degeneracy factor $(2J+1)$ against CO_2 rotational energy. This experiment was done in a background subtraction manner with and without the excitation laser pulse. The linearity of the plot established the Boltzmann form for the rotational distributions. The rotational temperatures are $T_{rot}=608\pm48$ K for $v''=14$ and 818 ± 65 K for $v''=21$, respectively. The rotational temperatures of CO_2 $(00^{0}0)$ in high rotational states populated by collisions with highly vibrationally excited KH($v''=14$–21) are listed in Table 2. Based on rotational temperatures, the average

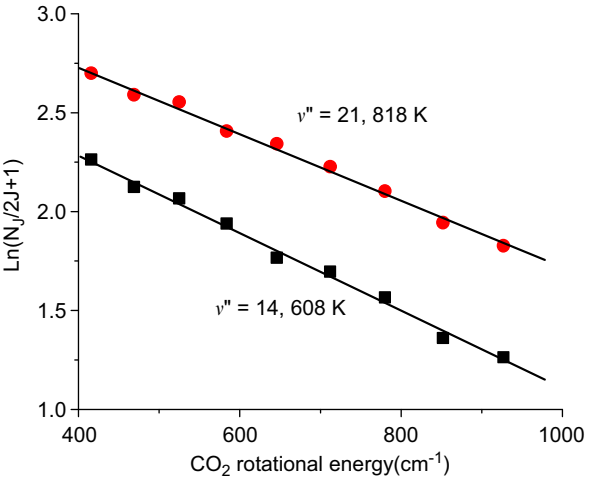

Fig. 7. Nascent distributions of CO_2 $(00^{0}0)$ in high rotational states $J\sim32$–48 populated by collisions with highly vibrationally excited KH ($X^1\Sigma^+$) initially prepared with $v''=14$ and 21; CO_2 populations were measured at $t=1$ μs following excitation of KH.

rotational energy of CO_2 molecules (with $J\geq32$) increases by nearly a factor of 1.35 when the KH internal energy increases by a factor of 1.27.The average change in the CO_2 rotational energy $\langle\Delta E_{rot}\rangle$ has a stronger dependence on the KH internal energy. $\langle\Delta E_{rot}\rangle$ is determined from $\langle\Delta E_{rot}\rangle=k_B(T_{rot}-T_0)$, where T_0 describes the initial rotational distribution. Using the ambient cell temperature for T_0, we find that $\langle\Delta E_{rot}\rangle_{v''=21}\approx2.33\langle\Delta E_{rot}\rangle_{v''=14}$.

Translational energy release from KH (v'')–CO_2 collisions

The nascent distributions of recoil velocities for collisions were determined from LIF line profiles of individual CO_2 rotational states. LIF line shapes for the CO_2 $(00^{0}0)$ $J=40$ are shown in Fig. 8, when $v''=14$ and 20 were prepared. For $v''=14$, Fig. 8a shows the full width at

Table 2
Rotational temperatures of CO_2 (00^00) in high rotational states populated by collisions with highly vibrationally excited KH($X^1\Sigma^+$,v'') states.

v''	14	15	16	17	18	19	20	21
T_{rot} (K)	608 ± 48	629 ± 50	641 ± 52	649 ± 54	728 ± 60	750 ± 62	802 ± 63	818 ± 65

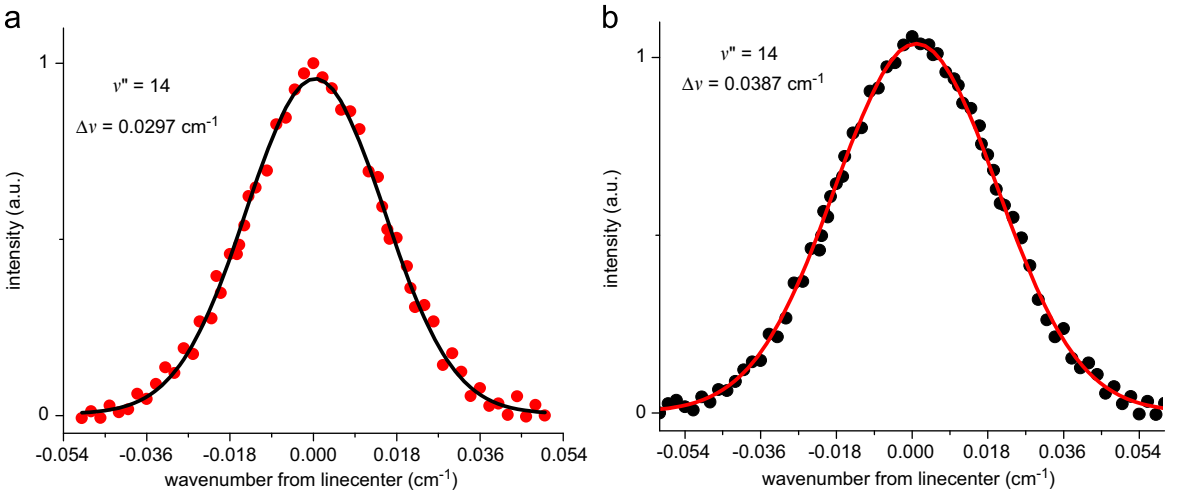

Fig. 8. Doppler-broadened transition line profiles for CO_2 (00^00) $J=40$ collected at $t=1$ μs following excitation of KH $v''=14$(a) and 20(b) ($P_{CO_2}=15$mTorr).

half-maximum (FWHM) linewidth of the $J=40$ state is $\Delta v=0.0297\ cm^{-1}$ which corresponds to a laboratory-frame velocity distribution with a temperature of $T_{trans}=555 \pm 89$ K. The laboratory frame translational temperature is determined using $T_{trans}=(mc^2/8\ k_B \ln 2)(\Delta v/v_0)^2$ in units K, where m is the mass of CO_2, and v_0 is rovibrational transition frequency at line center. For $v''=20$ (Fig. 8b), the nascent velocity distribution for the CO_2 $J=40$ state is broadened and has $T_{trans}=859 \pm 146$ K. The distribution of relative recoil energies for scattered KH and CO_2 is obtained by converting into the center of mass frame and is a measure of the amount of KH internal energy that goes into translation of the scattered molecules. Relative average translational energy is obtained by using $\langle E_{rel}\rangle=1.5\ k_B T_{rel}$, based on an isotropic velocity distribution. The center of mass translational temperature is determined using $T_{rel}=T_{trans}+(m_{CO_2}/m_{KH})(T_{trans}-T_0)$, where T_0 is taken to be the cell temperature. For KH ($v''=14$), the relative translational energy distribution for the CO_2 $J=40$ state has a temperature of $T_{rel}=673 \pm 113$ K, corresponding to an average translational energy $\langle E_{rel}\rangle=698 \pm 118\ cm^{-1}$. For KH ($v''=20$), the values increase to $T_{rel}=1309 \pm 223$ K and $\langle E_{rel}\rangle=1361 \pm 242\ cm^{-1}$ for $J=40$ state.

Fig. 9 shows post-collision $\langle E_{rel}\rangle$ values as a function of final CO_2 rotational state for quenching collision of KH $v''=14$ and $v''=20$. For both initial energies, the translational energy in the scattered molecules increases roughly linearly as a function of CO_2 J state for $J \geq 36$. The increase in translational energy of CO_2 J state shows that the relative velocity changes are accompanied by angular momentum increases as expected for impulsive collisional energy transfer. For KH ($v''=14$), scattered CO_2 molecules with $J=36$–48 have a center of mass translational energies of $\langle E_{rel}\rangle=535$–$1018\ cm^{-1}$. For KH ($v''=20$), the $J=36$–48 states of CO_2 have larger velocity distributions with $\langle E_{rel}\rangle=1075$–$1810\ cm^{-1}$. Average changes in translational energy $\langle \Delta E_{rel}\rangle$ for the scattered molecules also are dependent on donor energy. Values of $\langle \Delta E_{rel}\rangle$ are determined by using $\langle \Delta E_{rel}\rangle=1.5\ k_B(T_{rel}-T_0)$. For KH ($v''=14$), $\langle \Delta E_{rel}\rangle=67$–$550\ cm^{-1}$. For KH ($v''=20$), $\langle \Delta E_{rel}\rangle=607$–$1342\ cm^{-1}$, indicating that the strong collision is more impulsive for the higher energy donor.

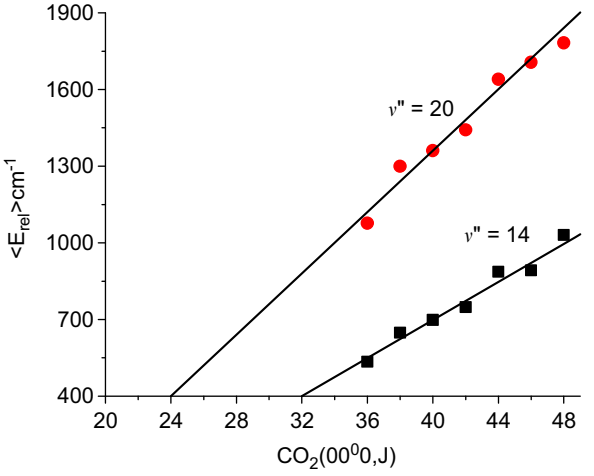

Fig. 9. CO_2 rotational state dependence of the average relative translational energy resulting from collisions with highly vibrational excited KH at $v''=14$ and $v''=20$.

Fig. 9 also shows that for KH ($v''=14$), the low-J CO_2 states are likely to have translational energy distributions that lie with a fairly narrow range with $\langle E_{rel}\rangle$ between 400 and 535 cm^{-1}. Extrapolating the data to the initial relative translational energy of $E_0=400\ cm^{-1}$ gives an estimate of the threshold state near $J\sim32$. For KH ($v''=20$) data, the low-J states of CO_2 have a large range of likely translational energies with values between $\langle E_{rel}\rangle\sim400$ and 1075 cm^{-1}. Extrapolation to the initial translational energy of $E_0=400\ cm^{-1}$ suggests that the minimum threshold J- state is near $J\sim24$. Of course, it is possible that a linear extrapolation to low-J state is not valid.

Rate coefficients of KH (v'')−$CO_2(00^00,J)$ energy transfer

Under single-collision conditions, the initial appearance rate of CO_2 (00^00, J) is due solely to collisions of KH (v'') with CO_2 and energy transfer rate coefficient k_J is determined using Eq. (4)

$$\frac{\Delta[CO_2(00^00,J)]}{\Delta t}=k_J[KH(v'')][CO_2] \tag{4}$$

here, $[CO_2]$ is the number density of CO_2; [KH (v'')] is the number density of KH (v'').

The Ti-sapphire laser (probe-laser) was reduced to typically 0.1 μW using neutral density filters, and the probe beam diameter was reduced to 1 mm at the center of the cell using a 1 m focal length lens and an aperture. Both pump- and probe-laser beams were well collimated over the length of the cell. We directly measure the [KH ($v''J''$)] number density by scanning the probe laser the $X^1\sum^+(v''J'')\rightarrow A^1\sum^+(v'J')$ transition and monitoring its transmission using PMT_2. In order to measure the spatial dependence [KH (v'', J'')] across the diameter of the cell, the probe laser was stepped across the diameter the cell, the probe laser was stepped across the cell parallel to the pump beam using the translating mirror shown in Fig. 1.

The transmitted intensity $I_\nu(L)$ of the probe-laser beam through a length L of the vapor is given by

$$\Delta I/I_\nu(0)=1-\exp[-k_{v'J'\leftarrow v''J''}(\nu)L] \tag{5}$$

for light of frequency ν. Here $\Delta I=I_\nu(0)-I_\nu(L)$, $I_\nu(0)$ is the incident intensity and $k_{v'J'\leftarrow v''J''}(\nu)$ is the frequency dependent absorption coefficient. [KH (v'', J'')] is related to the integral of $k_{v'J'\leftarrow v''J''}(\nu)$ by

$$\int k_{v'J'\leftarrow v''J''}(\nu)d\nu=\frac{[\lambda_{v'J'\rightarrow v''J''}]^2}{8\pi}\frac{g_{J'}}{g_{J''}}[KH\ (v''J'')]\,\Gamma_{v'J'\rightarrow v''J''} \tag{6}$$

where $g_{J'}$ and $g_{J''}$ are the degeneracial of the J' and J'' states, respectialy. $\Gamma_{v'J'\rightarrow v''J''}$ is the natural radiation rate of the transition [21] and $\lambda_{v'J'\rightarrow v''J''}$ is the transition wavelangth. Thus we can extract [KH ($v''J''$)](x) from the position dependent probe transmission using Eqs. (5) and (6) (see Fig. 10).

If we assume that the [KH (14, 7)](x) was measured, from Fig. 3, [KH ($v''=14$)](x) is determined using Eq. (7)

$$[KH\ (v''=14)](x)=\sum\nolimits_{J''}[I(J'')/I(7)][KH\ (14,7)](x) \tag{7}$$

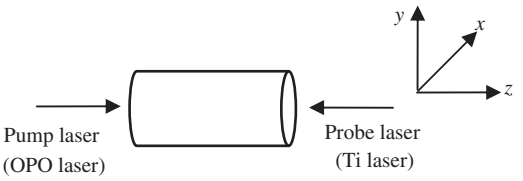

Fig. 10. The cell geometry and the measurement of spatial dependence [KH (v'')](x).

Table 3
Average densities (in $10^7\ cm^{-3}$) of KH ($v''=14$–21).

v''	14	15	16	17	18	19	20	21
$\overline{[KH\ (v'')]}$	1.1	1.3	1.2	0.8	0.7	0.5	0.4	0.6

The excited [KH (v'')](x) is numerically integrated over cell diameter to yield the average density

$$\overline{[KH\ (v'')]}=\int_{-R}^{R}[KH\ (v'')](x)dx/2R \tag{8}$$

The average densities of excited KH ($v''=14$–21) are listed in Table 3.

The energy transfer rate coefficient for production of an individual state is measured directly as $\Delta CO_2(00^00,J)/\Delta t$ based on transient absorption date collected at $\Delta t=1$ μs following the KH (v'') excitation pulse (e.g., Fig. 7). Coefficients k_J change with internal energy of KH (v'') and are listed in Table 4.

The uncertainties in measurement of k_J are fairly large. Intensity ratios a/I_0 probably have an uncertainty of as much as 10%. We estimated the uncertainties of $\int_{-R}^{R}[KH\ (v'')](x)dx$ to be approxinately 28%. The uncertainty of $\Gamma_{v'J'\rightarrow v''J''}$ is10%. The largest source of statistial uncertainty in the rate coefficients is that due to $\Delta CO_2(00^00,J)/\Delta t$. They may be uncertain by as much as 30%. Considering these various sources of statistical uncertainty, we estimate overall errors of ∼40% in our measured V–R transfer rate coefficients.

In addition, systematic effects and uncertainties should also be considered. We must consider collisional transfer process

$$KH\ (v_1'')+H_2\rightarrow KH\ (v_2'')+H_2 \tag{9}$$

This process deduces the density of KH (v'') and can distort the apparent V–R transfer rate coefficients. The transfer rate coefficient of process is $\sim10^{-12}\ cm^3$ $molecule^{-1}\ s^{-1}$. In this experiment, the density of H_2 is $10^{14}\ cm^{-3}$. KH (v'')→H_2 transfer contributes 10% uncertainty to our rate coefficients. We must also consider collisional transfer process

$$CO_2(00^00,J)+CO_2\rightarrow CO_2(00^00,J')+CO_2 \tag{10}$$

If we assume an excitation transfer rate coefficient of $10^{-10}\ cm^3$ $molecule^{-1}\ s^{-1}$, then CO_2 gas pressure of 15 mTorr (∼$10^{15}\ cm^{-3}$ density) produces ∼10 μs collisitional lifetimes. For very short times (1 μs) following overtone excitation of KH, we estimate the uncertainty 10% due to neglect of $J\rightarrow J'$ transfer.

Considering only the statistical sources of uncertainties, we have determined values of the rate coefficients which is presented in Table 3. However, the accuracy of

Table 4
Energy transfer rate coefficients for collisions of highly excited KH with CO_2.

$CO_2(00^00,J)$	KH (v'')							
	14	15	16	17	18	19	20	21
	$k_J(\times 10^{-13}$ cm^3 molecule^{-1} s$^{-1})$							
32	1.37 ± 0.55	1.51 ± 0.60	1.62 ± 0.65	1.78 ± 0.71	2.45 ± 0.98	5.61 ± 2.24	3.72 ± 1.49	3.19 ± 1.28
34	1.28 ± 0.51	1.38 ± 0.55	1.50 ± 0.60	1.59 ± 0.64	2.29 ± 0.92	5.44 ± 2.18	3.58 ± 1.43	2.96 ± 1.18
36	1.16 ± 0.46	1.28 ± 0.51	1.38 ± 0.55	1.45 ± 0.58	2.09 ± 0.84	5.28 ± 2.11	3.36 ± 1.34	2.78 ± 1.11
38	1.06 ± 0.42	1.17 ± 0.47	1.20 ± 0.48	1.33 ± 0.53	1.90 ± 0.76	4.73 ± 1.89	3.21 ± 1.28	2.67 ± 1.07
40	0.95 ± 0.38	1.03 ± 0.41	1.11 ± 0.44	1.24 ± 0.50	1.77 ± 0.71	4.19 ± 1.68	2.98 ± 1.19	2.55 ± 1.02
42	0.86 ± 0.34	0.80 ± 0.32	0.93 ± 0.37	1.14 ± 0.46	1.70 ± 0.68	3.92 ± 1.57	2.76 ± 1.10	2.36 ± 0.94
44	0.75 ± 0.30	0.77 ± 0.31	0.81 ± 0.32	0.99 ± 0.40	1.57 ± 0.63	3.65 ± 1.46	2.54 ± 1.02	2.24 ± 0.90
46	0.65 ± 0.26	0.73 ± 0.29	0.78 ± 0.31	0.89 ± 0.36	1.44 ± 0.58	3.29 ± 1.32	2.30 ± 0.92	2.03 ± 0.81
48	0.58 ± 0.23	0.67 ± 0.27	0.75 ± 0.30	0.82 ± 0.33	1.29 ± 0.52	3.04 ± 1.22	2.15 ± 0.86	1.88 ± 0.75
k_{int}[a]	8.66 ± 3.46	9.34 ± 3.74	10.08 ± 4.03	11.23 ± 4.49	16.50 ± 6.60	39.15 ± 15 .66	26.60 ± 10.64	22.66 ± 9.06

[a] Integrated bimolecular rate coefficient in 10^{-13} cm^3 molecule^{-1} s^{-1}.

these results may be limited by the systematic effects discussed above.

Conclusions

A dynamics study on the collisional energy transfer of highly vibrationally excited KH with CO_2 is presented. Three lasers are used. One is for production of KH, the second is used to prepare KH in the highly vibrational levels and the third probes the LIF signals initialed from scattered nascent CO_2 ($00^00, J$) states. The main results are the following.

(a) KH (v'') total relaxation rate coefficients for CO_2 for vibrational states up to $v''=21$ are measured accurately.
(b) The average rotational energy of scattered CO_2 (00^00, J) is increased by a factor of 2.33 when $v''=14$ state increases to $v''=21$. The average translational energy of scattered CO_2 ($00^00, J$) is increased roughly linearly as a function of J state.
(c) For $v''=19$, the integrated rate coefficients k_{int} increases by a factor of 4.5 to $v''=14$.

Acknowledgments

This work was supported by the National Natural Science Foundation of China under Grant No 10964011.

References

[1] Oref I, Tardy DC. Energy transfer in highly excited large polyatomic molecules. Chem Rev 1990;90:1407–45.
[2] Flynn GW, Parmenter CS, Wodtke AM. Vibrational energy transfer. J Phys Chem 1996;100:12817–38.
[3] Barker JR, Yoder LM, King KD. Vibrational energy transfer modeling of nonequilibrium Polyatomic Reaction Systems. J Phys Chem A 2001;105:796–809.
[4] Sery ET, Muyskens MA, Lin Z, Flynn GW. Competition between photochemistry and energy transfer in ultraviolet-excited diazabenzenes.3.photofragmentation and collisional quenching in mixtures of 2- methylpyrazine and carbon dioxide. J Phys Chem A 2000;104:10538–44.
[5] Park J, Shum L, Lemoff AS, Werner K, Mullin AS. Methylation effects in state-resolved quenching of highly vibrationally excited azabenzenes (Evib$\sim$38 500 cm^{-1}).II. Collisions with carbon dioxide. J Chem Phys 2002;117:5221–33.
[6] Mitchell DG, Johnson AM, Johnson JA, Judd KA, Kim K, Mayhew M, et al. Collisional relaxation of the three vibrationally excited difluorobenzene isomers by collisions with CO_2: effect of donor vibrational mode. J Phys Chem A 2008;112:1157–67.
[7] Park J, Li Z, Lemoff AS, Rossi C, Elioff MS, Mullin AS. Energy-dependent quantum-state-resolved relaxation of highly vibrationally excited pyridine (Evib=36 990–40 200 cm^{-1}) through collisions with CO_2. J Phys Chem A 2002;106:3642–50.
[8] Wall MC, Mullin AS. Supercollision energy dependence: state-resolved energy transfer in collisions between highly vibrationally excited pyrazine (Evib=37 900 cm^{-1} and 40 900 cm^{-1}) and CO_2. J Chem Phys 1998;108:9658–67.
[9] Wall MC, Lemoff AE, Mullin AS. Unraveling the energy dependence in large ΔE ($V\rightarrow RT$)energy transfer: Separation of ΔE and probability in the collisional relaxation of highly vibrationally excited pyrazine (Evib=36 000 to 41 000 cm^{-1})by CO_2. J Chem Phys 1999;111:7373–82.
[10] Yuan LW, Du J, Mullin AS. Energy-dependent dynamics of large-ΔE collisions: highly vibrationally excited azulene (E=20 390 and 38 580 cm^{-1}) with CO_2. J Chem Phys 2008;129:014303–1/11.
[11] Mack JA, Mikulecky K, Wodtke AM. Resonant vibration–vibration energy transfer between highly vibrationally excited O_2 ($X^3\sum g-$, v=15–26) and CO_2, N_2O, N_2, and O_3. J Chem Phys 1996;105:4105–16.
[12] Silva M, Jongma R, Field RW, Wodtke AM. The dynamics of stretched molecules: experimental studies of highly vibrationally excited molecules with stimulated emission pumping. Annu Rev Phys Chem 2001;52:811–51.
[13] Price JM, Mack JA, Rogaski CA, Wodtke AM. Vibrational-state-specific self-relaxation rate constant measurements of highly vibrationally excited O_2 (v=19–28). Chem Phys 1993;175:83–98.
[14] Park H, Slanger TG. O_2(X, v=8–22) 300 K quenching rate coefficients for O_2 and N_2, and $O_2(x)$ vibrational distribution from 248 nm O_3 photodissociation. J Chem Phys 1994;100:287–300.
[15] Wong TH, Kleiber PD, Yang KH. Chemical dynamics of the reaction K* ($5p^2P$)+H_2→KH(v=0; J)+H: electronic orbital alignment effects. J Chem Phys 1999;110:6743–8.
[16] Liu DK, Lin KC. State-specific reaction and product energy disposal of electronically excited potassium with hydrogen molecule. J Chem Phys 1997;107:4244–52.
[17] Liu DK, Lin KC. Rotational population distribution of KH (v=0, 1, 2, and 3) in the reaction of K (52 PJ, 62 PJ, and 72 PJ) with H_2: reaction mechanism and product energy disposal. J Chem Phys 1996;105:9121–9.
[18] Stwalley WC, Zemke WT, Yang SC. Spectroscopy and structure of the alkali hydride diatomic molecules and their ions. J Phys Chem Ref Date 1991;20:153–87.
[19] Campargue A, Bailly D, Teffo JL, Tashkun SA, Perevalov VI. The $\nu_1+\nu_3$ Dyad of $^{12}CO_2$ and $^{13}CO_2$. J Mol Spectrosc 1999;193:204–12.
[20] Lucchesini A, Gozzini S. Diode laser overtone spectroscopy of CO_2 at 780 nm. J Quant Spectrosc Radiat Transf 2005;96:289–99.
[21] Giroud M, Nedelec O. Lifetimes and collisions in KH, $A^1\sum+$, v'=5–22. J Chem Phys 1982;77:3998–4005.